IL NUOVO CIMENTO Vol. 35 C, N. 5 Settembre-Ottobre 2012
DOI 10.1393/ncc/i2012-11315-5

Communications: SIF Congress 2011

Mu-Steel: Muon tomography for environmental protection

M. Furlan(*)

Università di Padova - via F. Marzolo 8, 35131 Padova (PD), Italy
INFN, Sezione di Padova - via F. Marzolo 8, 35131 Padova (PD), Italy

ricevuto il 29 Dicembre 2011; approvato il 12 Marzo 2012

Summary. — The accidental melting of radioactive sources hidden inside metal scrap containers can produce severe environmental harm. The muon tomography is a technique that allows to discriminate high-Z materials through cosmic-ray muons multiple scattering inside matter. A European project to exploit this technique to detect the presence of shielded radioactive sources was approved in 2010. In this paper some details of the project are presented, highlighting the scientific and technological aspects.

PACS 89.60.-k – Environmental studies.
PACS 89.20.-a – Interdisciplinary applications of physics.

1. – Introduction

The steel industry makes large use of scrap metal in the recycling phase. A known concern in the process is the possibility that a radioactive source (called "orphan" source) can be hidden inside the cargo. The melting of a radiosource can produce environment contamination and large economic losses.

To reduce the risk, modern recycling plants host radiation scanning portals. However, if the source is well shielded (*e.g.*, sealed inside a lead container), radiation detectors fail to detect it and accidental melting can occur.

Muon tomography has been proposed as a tool to detect not the radioactive material itself but rather its heavy metal shielding. The combined examination through a radiation portal and a muon tomography scanner can therefore eliminate the risk.

Muon tomography makes use of cosmic-ray muons to build a high-density material sensible 3D map of the examined volume. To be effective, a large number of muons must be collected. This can conflict with the requirements of the recycling process, that limits the analysis time of the scrap metal cargo to a few minutes at most.

(*) E-mail: matteo.furlan@pd.infn.it

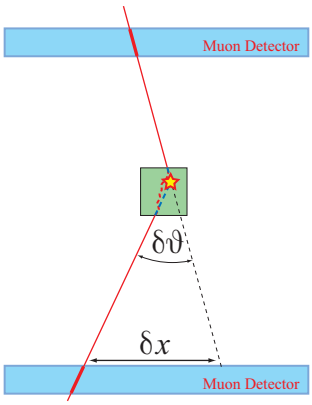

Fig. 1. – The variables measured in the scattering process.

2. – Muon tomography technique

Muon tomography [1] is based on Multiple Coulomb Scattering of charged particles. When a charged particle crosses a material, its trajectory is deflected from the direction of incidence. The distribution of the scattering angle ($\delta\theta$) projected on a plane containing the incident particle trajectory is approximately Gaussian with zero mean and variance related to the properties of the homogeneous crossed volume [5-7]:

$$\sigma^2 = \frac{(13.6\,\mathrm{MeV}/c)^2}{\beta^2 p^2}\frac{L}{X_0}\left[1 + 0.038\log\left(\frac{L}{X_0}\right)\right]^2 \simeq \frac{(13.6\,\mathrm{MeV}/c)^2}{p^2}\frac{L}{X_0}\,, \tag{1}$$

where L is the crossed material thickness, X_0 its radiation length and p is the particle momentum and β its velocity. Measuring the deflection of many particles is therefore possible to infer the quantity

$$\lambda = \frac{1}{X_0} = \rho \cdot \left[\frac{Z(Z+1)\log(287/\sqrt{Z})}{A \cdot 716.4\,\mathrm{g/cm^2}}\right], \tag{2}$$

to which we will refer as "scattering density" in the present paper. As can be seen from eq. (2), it is strongly related to mass density. The projections of the scattering angle on two orthogonal planes are statistically independent. The displacement δx (fig. 1) is correlated to the scattering angle and contributes significantly to the resolution of the system since it contains information on spatial position of the scattering point.

Cosmic rays are a rich source of charged particles [8]. They are originated by protons and alpha-particles interacting with the high atmosphere and generating showers of particles. At sea level the showers are composed primarily by muons with a rate of $\sim 100\,\mathrm{Hz/m^2}$. Their momentum spectrum $g(p)$ is quite broad.

The aim of the muon tomography is to obtain a three-dimensional map of the density distribution inside a non-homogeneous volume. This can be represented by a collection of homogeneous subvolumes (voxels), whose dimensions are related to the resolution of the final image. The total variance of the scattering of the i-th muon through N voxels

can be written as a function of the voxel scattering density and path length L_{ij} of the i-th muon inside the j-th voxel:

$$\sigma_i^2 = \frac{(13.6\,\mathrm{MeV}/c)^2}{p^2} \sum_{j=1}^{N} L_{ij}\lambda_j. \tag{3}$$

Therefore, it is necessary to gather the largest amount possible of muons in order to obtain a precise value for the variance.

To obtain the scattering angle it is necessary to measure the particle trajectory before it enters and after it exits the considered volume.

This suggests a first approach to obtain information about the distribution of density inside the volume. In fact, in the Single Scattering Point Approximation (SSPA), a map of the scattering points can be built intersecting the entering and exiting particle trajectory, identifying the Points of Closest Approach (PoCA). The SSPA is quite crude and it behaves badly when the particle undergoes more than a single important scattering.

Since in our application the measure of the muon momentum is not feasible, the scattering angle distribution due to the crossing of a given material thickness L must be written as the convolution([1]):

$$f(\delta\theta) \propto \sqrt{\frac{X_0}{2\pi L}} \int_0^\infty g(p) \exp\left[-\frac{\delta\theta^2}{2\sigma^2(p)} \right] p\mathrm{d}p. \tag{4}$$

The computational weight of the evaluation of such an integral could be overwhelming for a reconstruction software. The spectrum $g(p)$ is therefore approximated by an "effective" momentum value, $p_{\mathrm{eff}} \sim 700\,\mathrm{MeV}$ and the variance in eq. (3) becomes

$$\sigma_i^2 = k \sum_{j=1}^{N} L_{ij}\lambda_j, \qquad k = \frac{(13.6\,\mathrm{MeV}/c)^2}{p_{\mathrm{eff}}^2}\,. \tag{5}$$

This approximation will lead to a degree of noise of the reconstructed image.

To build a useful 3D map, the contribution of the largest possible set of muons must be collected, covering different positions and trajectory angles in the reconstructed volume. From eq. (4) and eq. (3) one can write the likelihood of occurrence of the scattering angles measured in the sample of M muons as a function of the density profile $\underline{\lambda} = \lambda_1, \lambda_2, \ldots, \lambda_N$:

$$P(\underline{\lambda}) = \prod_{i=1}^{M} \frac{1}{\sigma_i(\underline{\lambda})\sqrt{2\pi}} \exp\left[-\frac{\delta\theta_i^2}{2\sigma_i^2(\underline{\lambda})} \right]. \tag{6}$$

Thus it is possible to build the density profile $\underline{\lambda}$ in the volume by minimizing the logarithmic likelihood

$$\ln P(\underline{\lambda}) = -\sum_{i=1}^{M} \left[\frac{\delta\theta_i^2}{2\sigma_i^2(\underline{\lambda})} + \ln(\sigma_i(\underline{\lambda})) \right], \tag{7}$$

([1]) The displacement δ has been omitted from the equations in the present paper to ease the notation.

Fig. 2. – The scanning portal prototype at LNL. The two muon drift chambers are spare units of the muon chambers built for the CMS experiment.

that is equivalent to maximize the function

$$\Psi\left(\underline{\lambda}\right) = \sum_{i=1}^{M} \left[\frac{\delta\theta_i^2}{k \sum_{j=1}^{N} L_{ij}\lambda_j} + \ln\left(\sum_{j=1}^{N} L_{ij}\lambda_j \right) \right], \tag{8}$$

in the set of N variables $\underline{\lambda}$. This is achieved through an iterative Expectation Maximization (EM) algorithm [2, 3].

3. – Experimental set-up

The INFN Laboratori Nazionali di Legnaro host a large-size working prototype of a scanning portal, represented in fig. 2.

A volume of about $3.00\,\mathrm{m} \times 2.40\,\mathrm{m} \times 1.60\,\mathrm{m} = 11.5\,\mathrm{m}^3$ included between two muon drift chambers can be used for test inspections. The two detectors, above and below, measure the trajectories respectively for each incoming and outgoing particle. The chambers are spare units of the barrel muon chambers of the CMS experiment. Each detector is made of twelve wire layers, eight of which measure the θ angles and x position, while the remaining four measure the orthogonal variables ϕ and z. The precision of these detectors, namely $200\,\mu\mathrm{m}$ in position, $\sim 2\,\mathrm{mrad}$ in θ angle and $\sim 10\,\mathrm{mrad}$ in ϕ is quite better than required for the projects purposes [9]. Inside the space between the chambers it is possible to place different sets of objects to be scanned. The set proposed for the images presented in this paper is shown in fig. 3.

Four lead blocks placed on top of the lower chamber act as a reference for position and crosscheck of the reconstructed scattering density value. At the center of the volume, a structure made of two $1.00\,\mathrm{m} \times 0.8\,\mathrm{m} \times 0.15\,\mathrm{m}$ iron slabs separated by about $0.3\,\mathrm{m}$ is present. The slab total thickness has a radiation length equivalent to that of a real-sized container filled with metal scrap. Inside the slabs, a $0.25\,\mathrm{m} \times 0.25\,\mathrm{m} \times 0.2\,\mathrm{m}$ lead block represents the shielded source.

Fig. 3. – The structure analyzed. Three of the four lead blocks used as reference can be seen.

4. – Timing constraints and workloads

One of the major constraints for the scanning and material identification process is processing time. Its direct industrial application requires that a truck must be inspected and the portal cleared out in a few minutes. A time of $\sim 300\,\mathrm{s}$ will be assumed. This has two main implications. The first concerns the total number of muons that can be collected in such a time. A low muon count will generate a lot of statistical noise in the final image, due to the statistical nature of the reconstruction process. The second implication is that the computational time must be rigidly optimized to fit in the acquisition chain schedule.

In the EM muon tomographic process the number of voxels is the number of variables in the minimization function. The volume of the final portal will be of about $\sim 350\,\mathrm{m}^3$. This must be divided in a number of voxels that is lower-bounded by the requested resolution and upper-bounded by the acquired statistics. Hence it is reasonable to expect a very high number of voxels and hence of variables. It can be estimated in 10^6 to 10^7 voxels when taken of reasonable size, namely around 5 cm per edge. With a rate of $100\,\mathrm{Hz/m}^2$, in the given time the collected muons are of order $\sim 10^6$. It is evident that the reconstruction software must work on a massive amount of data in a relatively small time.

The previous version of the reconstruction software, while already well performing, was not quite adequate to achieve the requested performance. An optimization has been performed to shorten the reconstruction time. The benchmark has been performed in the working condition presented in table I. The voxels have been taken of the same reasonable edge sized as intended for the portal. A resulting image, obtained with a higher statistics with respect to the benchmark, is shown in fig. 4. The lead "shield" is clearly visible between the iron slabs with a density similar to that of the reference blocks.

TABLE I. – *Default testing condition for the algorithm.*

Processing load	
Muons	$1 \cdot 10^6$
Voxels	$3.44 \cdot 10^4$
Iterations	$5 \cdot 10^2$

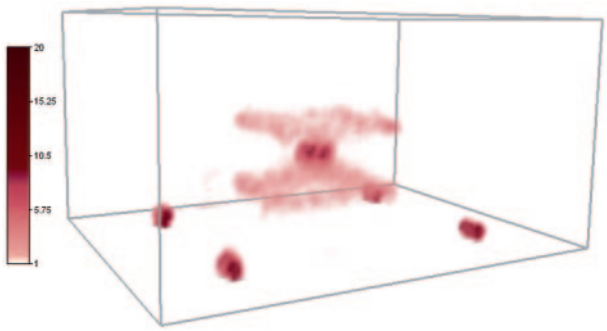

Fig. 4. – A tomographic image obtained from real measurements of cosmic-ray muons.

5. – Optimization and benchmarking

All the programs developed for this project have been written in C/C++. The performance of our software has been enhanced by working on two directions. The first is memory management and cache optimization. The second is implementing parallel processing capabilities.

5˙1. *Memory management.* – Objects created with C++ load to memory bits of code that, in some applications, are not required. The data structures implemented as objects that did not require inheritance or dedicated access members have been turned to C structures. Loops have been lightened to perform the minimum number of operations. Most of the variables shared by different portion of the code have been passed through reference and not by copy, to cancel the time required to replicate data in memory. For the extent that was achievable through a user-space–oriented programming, data have been grouped and disposed sequentially, in order to improve the performance of the CAS-line–based memory fetching mechanism. The sizes in memory of the most frequently used structures have been adapted to fit inside cache pages. Moreover, the 'if' statements inside loops that, *a priori*, were known to be less probably executed, have been optimized not to be loaded in the instruction cache.

All the presented methodologies allow a better usage of the "dead time" of the processor, that often needs to wait for the memory controller to fetch data from RAM and clean and refill its workbench, the cache.

5˙2. *Parallel processing support.* – Giving parallel processing capability to a loop-based algorithm is pretty straightforward. Nonetheless, one must take some care in order to make the most of parallelization. The algorithm has been slightly rearranged to minimize thread "waiting" and concurrency memory locks. The specific algorithm suffers those issues. While iteration must occur sequentially, the muons processing can occur in parallel. Nonetheless, every intermediate step of the single iteration requires all the muons gathered information. Therefore, threads must wait for each other to complete before proceeding. This is intrinsic with the procedure and it may not have a solution.

5˙3. *Results.* – The amount of improvement in processing times obtained through the named optimization have been tested using the condition in table I. The original edition of the program gives the results in table II. After the rewriting of the code following the optimization flow, the results are those presented in table III. The machine used is the

TABLE II. – *Results of the benchmarking of the first edition of the image reconstruction software.*

First Version	
Cores	1
Frequency	3.41 GHz
Memory	8 Gb
ETA	1860 s

same for both test. The reason for the quite large difference in clock frequency is due to the modern "power scaling" technology: when a single core is used instead of multiple cores, the power usually divided among all cores can be conveyed to the single core in use to gain clock frequency while keeping consumption (and temperature) under control.

5˙4. *Further development*. – More improvements are planned ahead, pushing further both directions of software performace enhancement pursued to reach the present result. The software will be partly rewritten and partly optimized in order to run over GPU-based computational devices. This is the next step in parallel processing development of the software. Modern GPU devices are able to crunch 10^3–10^4 threads at a times, so potentially drastically reducing the computational time.

On the memory management side the possibility is under study to build a low-level software driver able to reserve and organize the area of memory needed by the software, without the participation of the operative system.

Speed and performance is not the only direction the actual software must evolve to. The approximation of the function to be minimized (eq. (4) to eq. (6)) and the scarce number of muons that can be gathered in the little given time are a treacherous source of noise. Noise in a tomographic image can mislead the algorithm converging to a wrong scattering density inside some of the voxels. Its effect can be seen in the high statistic image presented in fig. 4. It generates "spikes" of high scattering density, that could lead to false identifications of high density materials presence. An accurate study over the best filtering method of the image is in progress at the moment, and filtering seems, by now, the best direction to take in image quality improvement.

Moreover, the sophisticated high-density–material identification algorithm must be implemented. At the moment only a simple and rough threshold algorithm is in working condition. This is necessary not only to complete the identification process chain, but also to evaluate the detecting efficiency of the system.

TABLE III. – *Results of the benchmarking of the second edition of the image reconstruction software.*

Second Version	
Cores	4
Frequency	2.93 GHz
Memory	8 Gb
ETA	97 s

6. – Conclusions

The results presented show that the muon tomographic reconstruction process already works. A 3D density map of a volume can be built using the Multiple Coulomb Scattering of cosmic-ray muons tracked by muons detectors. The analysis of the corresponding image can lead to the identification of a high-density material hidden inside several radiation lengths of iron.

In addition, the achieved results in algorithm speed optimization are quite impressive. The processing time has dropped by a factor ~ 20. It is an important step towards the building of a software capable to deliver production level results. Further developments are in progress.

* * *

The *Mu-Steel* project is carried out with a grant of the European Commission within the Research Fund for Coal and Steel, RFSR-CT-2010-000033. The research described in the present paper has been made possible by funding from the *Mu-Steel* project and from the University of Padova (Progetti di Ateneo 2009).

REFERENCES

[1] Borozdin K. N. *et al.*, *Nature*, **422** (2003) 277.
[2] Schultz L. J. *et al.*, *Nucl. Instrum. Methods A*, **519** (2004) 687.
[3] Schultz L. J. *et al.*, *IEEE Transaction on Image Processing*, Vol. **16**, No. 8 (2007) 1985.
[4] Dempster A., Laird N. and Rubin D., *J. R. Stat. Soc. B*, **39** (1977) 1.
[5] Moliere G. Z., *Z. Naturforsch A*, **2** (1947) 133.
[6] Moliere G. Z., *Z. Naturforsch A*, **3** (1948) 78.
[7] Bethe H. A., *Phys. Rev.*, **89** (1953) 1256.
[8] Rossi B., *High Energy Particles* (Prentice-Hall, Englewood Cliffs, NJ) 1952.
[9] Pesente S. *et al.*, *Nucl. Instrum. Methods A*, **604** (2009) 738.